Generalized oscillator strengths for the valence-shell excitations of neon

Hua-Dong Cheng, Lin-Fan Zhu,* Zhen-Sheng Yuan, Xiao-Jing Liu, Jian-Min Sun, Wei-Chun Jiang, and Ke-Zun Xu
Hefei National Laboratory for Physical Sciences at Microscale, Department of Modern Physics, University of Science and Technology of China, Hefei, Anhui, 230026, China
(Received 6 April 2005; published 22 July 2005)

The generalized oscillator strengths for the valence-shell excitations to $2p^5 3s$, $2p^5 3p$, and $2p^5 4s$ of neon were measured with an angle-resolved fast-electron energy-loss spectrometer at an incident electron energy of 2500 eV. The transition multipolarities for these excitations were elucidated with the help of the calculated intermediate-coupling coefficients using the COWAN code. The generalized oscillator strength profiles for the electric monopole, electric dipole, and electric quadrupole excitations were analyzed and their positions of the extrema were obtained. Furthermore, the experimental generalized oscillator strength ratios between the excitations to $2p^5 4s[3/2]_1$ and $2p^5 4s'[1/2]_1$ were determined and found to be in agreement with the calculated intermediate-coupling coefficient ratio.

DOI: 10.1103/PhysRevA.72.012715 PACS number(s): 34.80.Gs, 33.70.Fd, 31.15.Ne

I. INTRODUCTION

The electron impact excitation of neon is interesting from both the fundamental and applied points of view; e.g., the electron impact excitation mechanism of neon is extensively used in producing x-ray lasers [1,2]. The generalized oscillator strength (GOS) can be used to evaluate the theoretical methods, determine the correct spectral assignments [3], and explore the excitation dynamics [4]. The deviation of the magnitudes and positions of the minima or maxima of the GOS predicted by the theoretical calculations from the experimental results will serve as a test of the applicability of the Born approximation as well as the accuracy of the wave functions [5]. From our recent work [6], it is known that the GOS ratio is more direct and accurate to rigorously test the theoretical models than the GOS itself, and therein the valence-shell transition multipolarities of Kr for fast electron impact (e.g., electric monopole, electric dipole, and electric quadrupole) have been elucidated with the help of the calculated intermediate-coupling coefficients. To the best of our knowledge, the valence-shell transition multipolarities of Ne for fast electron impact have not been elucidated in previous experimental works.

In previous low-energy electron impact studies of Ne, Register *et al.* [7] measured the differential cross sections (DCS's) and the integrated cross sections (ICS's) for valence-shell excitations at incident electron energies of 25, 30, 50, and 100 eV. Recently, the DCS's and DCS ratios for the excitations to $2p^5 3s$ were measured and calculated at incident energies of 20, 25, 30, 40, 50, and 100 eV by Khakoo *et al.* [8–10]. For experiments with intermediate- and high-energy electron impact, Suzuki *et al.* [11] measured the DCS's and GOS's for excitations to $3s[3/2]_1$, $3s[1/2]_1$, and $3p'[1/2]_0$ at incident electron energies of 300, 400, and 500 eV. Wong *et al.* [12] observed the minima and maxima in the GOS's for the $np \rightarrow (n+1)s$ transition of noble gases at an incident electron energy of 25 keV.

Many theoretical works have been carried out to investigate the electron impact inelastic scattering of Ne. Ganas and Green [13] calculated the GOS's for the excitations to $2p^5 3s$ within the framework of the Born approximation. In order to study the effects of the distortion and exchange at low impact energies, Sawada *et al.* [14] reported the GOS's and ICS's for excitations to $2p^5 3s$ within the framework of the distorted Born approximation. Machado *et al.* [15] calculated the DCS's and ICS's for all excitations to $2p^5 3s$ and some of the excitations to $2p^5 3p$ levels of Ne using first-order many-body theory (FOMBT). Bartschat and Madison [16] calculated the nonstatistical branching ratios for excitations to $np^5(n+1)s$ of noble atoms by the relativistic distorted-wave Born approximation. Recently, Chen and Msezane [17] calculated the minima and maxima of the GOS's for excitations to $np^5(n+1)s$ of Ne ($n=2$), Kr ($n=4$), and Xe ($n=5$), and Amusia *et al.* [18] calculated the GOS's for the quadrupole and monopole transitions of $np \rightarrow (n+1)p, (n+2)p$ levels of noble atoms using the Hartree-Fock approximation (HFA) and the random phase approximation with exchange (RPAE).

With the above survey, it is noticed that most of the works concentrate on low-energy electron impact, in which transitions between states with different spin multiplicities are possible as a result of electron exchange effects [19]. However, for sufficiently fast electron impact, the influence of the incident particle upon an atom or molecule can be regarded as a sudden and small external perturbation. Thus the cross section can be factorized into two factors, one dealing with the incident particle only, the other (GOS) dealing with the target only, and the exchange effect is negligibly small [19]. The GOS was defined as [19–21] (in atomic units)

$$f(E,K) = \frac{E}{2}\frac{p_0}{p_a}K^2\frac{d\sigma}{d\Omega} = \frac{2E}{K^2}\left|\langle\Psi_n|\sum_{j=1}^{N}\exp(i\mathbf{K}\cdot\mathbf{r}_j)|\Psi_0\rangle\right|^2, \quad (1)$$

where E is the excitation energy, K is the momentum transfer, and p_0 and p_a are the incident and scattered electron momenta, respectively. $f(E,K)$ and $d\sigma/d\Omega$ stand for GOS

*Corresponding author. Electronic address: lfzhu@ustc.edu.cn

and DCS while Ψ_0 and Ψ_n are N electrons wave functions for initial and final states, respectively. $\mathbf{r}_j$ is the position vector of the jth electron.

In the present work, the GOS's for the valence-shell excitations to $2p^5 3s$, $2p^5 3p$, and $2p^5 4s$ of neon were measured at an incident electron energy of 2500 eV. The transition multipolarities for these excitations were elucidated with the help of our calculated intermediate-coupling coefficients using the COWAN code [22]. The GOS profiles for these excitations were analyzed, and the positions of the extrema were determined. The GOS ratios between the excitations to $4s[3/2]_1$ and $4s'[1/2]_1$ were determined and compared with the calculated results.

II. EXPERIMENTAL AND THEORETICAL METHODS

A. Experimental method

The angle-resolved electron-energy-loss spectrometer (AREELS) used in this experiment has been described in detail in Refs. [23–25]. Briefly, it consists of an electron gun, a hemispherical electrostatic monochromator made of aluminum, a rotatable energy analyzer of the same type, an interaction chamber, a number of cylindrical electrostatic lenses, and a one-dimensional position-sensitive detector for detecting the scattered electrons. All of these components are enclosed in four separate vacuum chambers made of stainless steel. The impact energy of the spectrometer can be varied from 1 to 5 keV. For the present measurement the impact energy was set at 2500 eV and the energy resolution was 70 meV [full width at half maximum (FWHM)]. The background pressure in the vacuum chamber was 5×10^{-5} Pa. The scattering angle was calibrated by the angular distribution of the $2p^6\rightarrow 2p^5(3s+3s')$ inelastic scattering signal around the geometry nominal 0°. The angular resolution was about 0.8° (FWHM) under the present experimental conditions.

In order to reduce the errors and improve the efficiency of the experimental measurement, a mixed gas of He and Ne with a fixed proportion was used to determine the relative excitation cross section of Ne by taking He as a standard. Here a gas cell was used and the electron collision lengths for He and Ne were identical. Thus the correction for the profile of the gas beam was not required. In addition, using the method of gas mixture, corrections to the angular factor and the intensity instability of the incident electron beam were not required either. The detailed measurement and correction procedures are described in the following.

In the present work, the electron-energy-loss spectra in the energy-loss region of 16–24 eV for Ne+He were measured from 0.5° to 8.5°. A typical electron-energy-loss spectrum is shown in Fig. 1, where the peaks from A to F of neon are labeled. The peaks G and H correspond to the excitations to $3\,^1S$ and $3\,^1P$ of helium, respectively, which are used to calibrate the data.

It is well known that the double-scattering processes can cause large errors in DCS measurements [24,26]. Because the intensity of double scattering is proportional to the square of the pressure, while the intensity of single scattering is proportional to the pressure, the relation between the measured intensity ratios and the pressure is

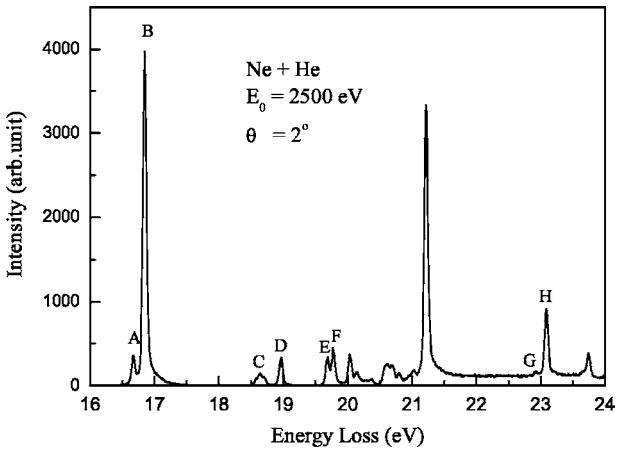

FIG. 1. A typical electron-energy-loss spectrum of Ne+He at the impact energy of 2500 eV and scattering angle of 2°.

$$\frac{I_p(\theta)}{I_{ref}(\theta)} \approx \left(\frac{I_p(\theta)}{I_{ref}(\theta)}\right)_{P=0} + c(\theta)P, \tag{2}$$

where $c(\theta)$ is a coefficient which depends on the scattering angle and the corresponding elastic and inelastic cross sections of He and Ne [27]. $I_p(\theta)$ and $I_{ref}(\theta)$ represent the intensity of the inelastic excitation of Ne and the intensity of the excitation to $3\,^1S+3\,^1P$ of helium, respectively. The values of $[I_p(\theta)/I_{ref}(\theta)]_{P=0}$, which are proportional to the corresponding ratios of cross sections, were obtained by a linear least-squares fitting [26]. In addition, the angular resolution has a great influence on the measurement of GOS's at small angles. Using the method described in Ref. [28], the influence of angular resolution was corrected for the GOS's at small angles.

The intensity ratio $[I_{\mathrm{Ne}}(\theta)/I_{\mathrm{He}}(\theta)]_{P=0}$ was calibrated with the DCS's of the excitations to $3\,^1S+3\,^1P$ of He calculated by Cann and Thakkar [29], which are in excellent agreement with our previous experimental results [30]. Then the relative DCS's for the valence-shell excitations of Ne can be determined. According to Eq. (1), the relative GOS's were obtained. Based on the Lassettre's limit theorem [31], it is known that the GOS converges to the optical oscillator strength (OOS) as $K^2\rightarrow 0$. The behavior of the GOS near $K^2=0$ is illustrated as

$$f(E_0,K) = \frac{1}{(1+x)^6}\left[f_0 + \sum_{n=1}^{m} f_k\left(\frac{x}{1+x}\right)^n\right], \tag{3}$$

where f_0 is the OOS and f_k are the fitted constants, $x=K^2/\alpha^2$ with $\alpha=(2I)^{1/2}+[2(I-E)]^{1/2}$, and I and E are the ionization and excitation energies, respectively. By fitting the relative GOS of the dipole-allowed excitation to $3s'[3/2]_1$

TABLE I. The intermediate-coupling coefficients and the assignments for peaks from *A* to *F*. The energy levels from Moore [35] and from our calculations are given. *E*0, *E*1, *E*2, *M*1, and *T* represent the electric monopole, electric dipole, electric quadrupole, magnetic dipole, and spin-forbidden transitions from the ground state($2p^6\ ^1S_0$), respectively.

Peak	*JL* designation	Intermediate coupling	Transition	Energy (eV) COWAN	Energy (eV) Moore
	$2p^6$	$0.9959(2p^6\ ^1S_0)$		0.000	0.000
	$2p^53s[3/2]_2$	$0.9998(2p^53s\ ^3P_2)$	*T*	16.560	16.619
A	$2p^53s[3/2]_1$	$0.9630(2p^53s\ ^3P_1)+0.2690(2p^53s\ ^1P_1)$	*E*1	16.611	16.671
	$2p^53s'[1/2]_0$	$0.9998(2p^53s\ ^3P_0)$	*T*	16.655	16.715
B	$2p^53s'[1/2]_1$	$-0.2690(2p^53s\ ^3P_1)+0.9627(2p^53s\ ^1P_1)$	*E*1	16.784	16.848
	$2p^53p[1/2]_1$	$-0.1299(2p^53p\ ^3P_1)+0.9858(2p^53p\ ^3S_1)$	*T*	18.407	18.382
	$2p^53p[1/2]_0$	$0.9959(2p^53p\ ^3P_0)$	*T*	18.687	18.711
	$2p^53p[5/2]_3$	$0.9999(2p^53p\ ^3D_3)$	*T*	18.532	18.555
	$2p^53p[5/2]_2$	$0.87122(2p^53p\ ^3D_2)-0.1561(2p^53p\ ^3P_2)+0.4652(2p^53p\ ^1D_2)$	*E*2	18.553	18.576
C	$2p^53p[3/2]_2$	$-0.2413(2p^53p\ ^3D_2)+0.6891(2p^53p\ ^3P_2)+0.6832(2p^53p\ ^1D_2)$	*E*2	18.612	18.637
	$2p^53p'[3/2]_2$	$0.4272(2p^53p\ ^3D_2)+0.7075(2p^53p\ ^3P_2)-0.5629(2p^53p\ ^1D_2)$	*E*2	18.678	18.704
	$2p^53p[3/2]_1$	$0.8398(2p^53p\ ^3D_1)-0.3165(2p^53p\ ^3P_1)-0.4408(2p^53p\ ^1P_1)$	*M*1	18.588	18.613
	$2p^53p'[3/2]_1$	$0.5426(2p^53p\ ^3D_1)+0.4805(2p^53p\ ^3P_1)+0.6888(2p^53p\ ^1P_1)$	*M*1	18.666	18.693
	$2p^53p'[1/2]_1$	$0.8074(2p^53p\ ^3P_1)+0.1566(2p^53p\ ^3S_1)-0.5686(2p^53p\ ^1P_1)$	*M*1	18.699	18.726
D	$2p^53p'[1/2]_0$	$0.9452(2p^53p\ ^1S_0)-0.2690(2p^54p\ ^1S_0)-0.1165(2p^55p\ ^1S_0)$	*E*0	19.165	18.966
	$2p^54s[3/2]_2$	$0.9998(2p^54s\ ^3P_2)$	*T*	19.710	19.664
E	$2p^54s[3/2]_1$	$0.7370(2p^54s\ ^3P_1)+0.6754(2p^54s\ ^1P_1)$	*E*1	19.733	19.688
	$2p^54s'[1/2]_0$	$0.9996(2p^54s\ ^3P_0)$	*T*	19.806	19.761
F	$2p^54s'[1/2]_1$	$-0.6754(2p^54s\ ^3P_1)+0.7367(2p^54s\ ^1P_1)$	*E*1	19.823	19.780

using this Lassettre formula and normalizing the extrapolated result (relative OOS) to the absolute OOS (0.156) measured by dipole (e,e) method [32], the absolute GOS for the excitation to $3s'[3/2]_1$ can be determined. Then the GOS's for other valence-shell excitations can be obtained by making reference to the GOS of the excitation to $3s'[3/2]_1$.

The overall errors in this work come from the statistics of counts δ_s, the angular resolution determination for small angle δ_r, the pressure correction δ_p, and the normalizing procedure δ_n as well as the error resulting from the deconvolution procedure δ_d. In this work, the maximum of each error is δ_s=4% for the weakest transition, δ_r=5%, δ_p=3%, δ_n=5%, and δ_d=5%. The total maximum errors are less than 10%.

B. Calculational method

The calculations of the intermediate coupling coefficients for the lowest 18 levels of Ne were performed with the COWAN code [22]. The method of calculation was described in detail by Clark *et al.* [33,34], and here we summarized it briefly. The one-electron radial wave functions for each of the electron configurations with the Hartree-Fock method were first calculated so as to minimize the center-of-gravity energy of the configuration. Then the configuration interaction was included when calculating the Coulomb integrations between each pair of the configurations. The energy matrices were set up for each possible value of the total angular momentum *J*, and the eigenstates and eigenvalues are then obtained through diagonalizing each matrices on the given basis set.

For the present calculations a 22-configuration basis set was used, and the calculated excitation energies are consistent with the Moore levels [35] within 0.2 eV. The calculated intermediate-coupling coefficients and the energy levels are listed in Table I.

III. RESULTS AND DISCUSSION

From Table I we notice that there exits singlet and triplet *LS* components in the intermediate-coupling scheme. Since the probability for the spin-forbidden transition in connection with the electron-exchange effect is negligibly small for fast electron impact [19], the contributions of the excitations from the ground state of $^1S_0$ to the triplet components can be

TABLE II. The GOS's for peak *A*, *B*, *C*, *D*, *E*, and *F*. The numbers in square brackets denote the power of 10.

K^2 (a.u.)	*A* $3s[3/2]_1$	*B* $3s'[1/2]_1$	*C* $3p[5/2,3/2]_2+3p'[3/2]_2$	*D* $3p'[1/2]_0$	*E* $4s[3/2]_1$	*F* $4s'[1/2]_1$
0.019	1.19[−2]	1.58[−1]			1.34[−2]	1.72[−2]
0.061	1.16[−2]	1.44[−1]	2.25[−3]	2.22[−3]	1.21[−2]	1.55[−2]
0.13	1.00[−2]	1.33[−1]	4.92[−3]	5.38[−3]	1.15[−2]	1.50[−2]
0.23	9.58[−3]	1.22[−1]	8.68[−3]	1.09[−2]	1.12[−2]	1.51[−2]
0.35	7.55[−3]	1.03[−1]	1.20[−2]	1.49[−2]	1.03[−2]	1.23[−2]
0.50	5.43[−3]	8.47[−2]	1.76[−2]	2.15[−2]	8.36[−3]	1.06[−2]
0.69	3.24[−3]	5.49[−2]	1.59[−2]	2.07[−2]	5.96[−3]	7.13[−3]
0.89	2.09[−3]	3.42[−2]	1.34[−2]	1.83[−2]	3.73[−3]	4.77[−3]
1.13	1.30[−3]	1.96[−2]	9.79[−3]	1.56[−2]	2.35[−3]	2.93[−3]
1.40	5.47[−4]	9.71[−3]	6.09[−3]	1.07[−2]	1.24[−3]	1.72[−3]
1.69	4.44[−4]	6.77[−3]	4.09[−3]	7.49[−3]	8.32[−4]	1.05[−3]
2.01	2.78[−4]	5.07[−3]	2.43[−3]	5.39[−3]	6.47[−4]	6.59[−4]
2.36	2.13[−4]	3.17[−3]	1.34[−3]	3.85[−3]	2.64[−4]	4.00[−4]
2.73	2.09[−4]	3.25[−3]	9.44[−4]	2.73[−3]	2.56[−4]	4.77[−4]
3.13	2.41[−4]	4.91[−3]	5.22[−4]	2.49[−3]	4.62[−4]	4.48[−4]
3.57	3.28[−4]	5.65[−3]	4.43[−4]	2.32[−3]	3.98[−4]	5.35[−4]
4.03	2.93[−4]	3.57[−3]	2.93[−4]	1.57[−3]	2.53[−4]	4.39[−4]

neglected. Thus the excited states—e.g., $3s[3/2]_2$, $3s'[1/2]_0$, $3p[1/2]_{0,1}$, $3p[5/2]_3$, $4s[3/2]_2$, and $4s'[1/2]_0$—which only consist of the triplet components in the intermediate-coupling scheme (see Table I), were not observed in the present spectra. In addition, the excitations to $3p[3/2]_1$, $3p'[3/2]_1$, and $3p'[1/2]_1$, which correspond to the magnetic dipole excitations based on the singlet components in the intermediate-coupling scheme, should not appear in the present spectra [6,36]. Therefore, the observed transitions of Ne in our concerned energy region consist of the ones to $2p^5(3p,4p,5p)\ ^1S_0$, $2p^5(3s,4s)\ ^1P_1$, and $2p^53p\ ^1D_2$, which correspond to the electric monopole, electric dipole, and electric quadrupole excitations, respectively. Based upon above discussion, the transition multipolarities for *A*–*F* were assigned, as shown in Table I.

The GOS's for the dipole-allowed transitions to $3s[3/2]_1$ and $3s'[1/2]_1$ are listed in Table II and shown in Figs. 2 and 3, respectively. It can be seen that the GOS's measured by Suzuki *et al.* [11] at the incident electron energies of 300, 400, and 500 eV are generally lower than the present results. This may be attributed to the normalizing procedures. In their work, elastic scattering cross sections were used to normalize the data, and the extrapolated OOS's are 0.0106 for the excitation to $3s[3/2]_1$ and 0.137 for the excitation to $3s'[1/2]_1$. However, the present OOS for excitations to $3s[3/2]_1$ and $3s'[1/2]_1$ are 0.0124 and 0.156, respectively, which were determined in our previous work [32] and are in good agreement with other experimental results [37]. From Fig. 3 it can be seen that the maximum position of the GOS for the excitation to $3s'[1/2]_1$ decreases with the increasing

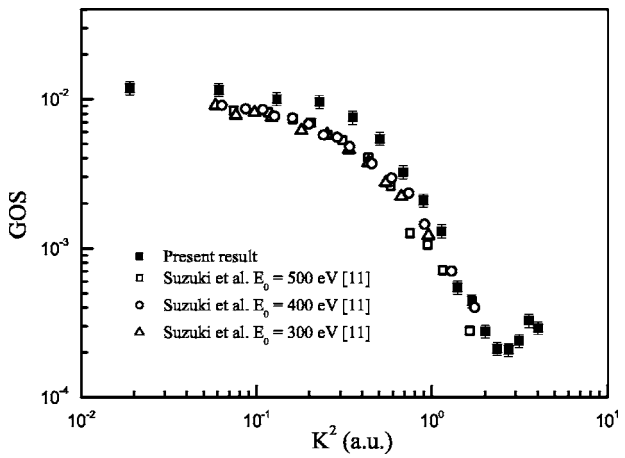

FIG. 2. The GOS for the electric dipole excitation to $3s[3/2]_1$.

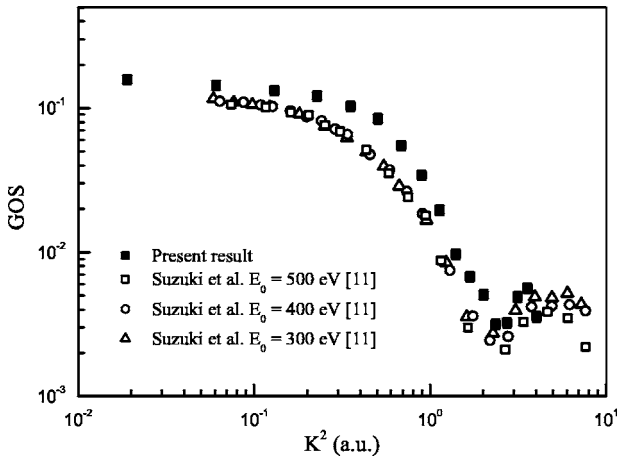

FIG. 3. The GOS for the electric dipole excitation to $3s'[1/2]_1$.

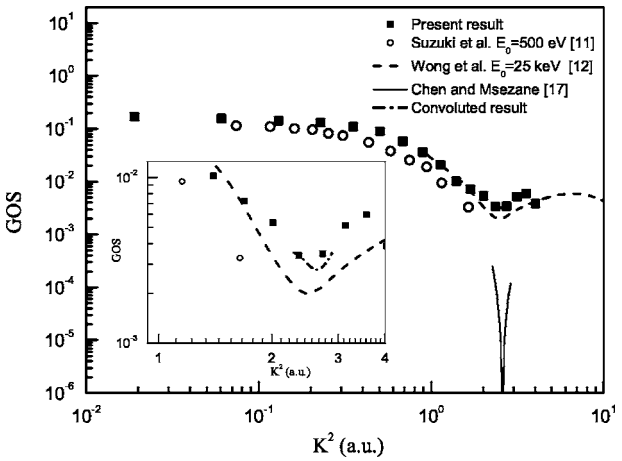

FIG. 4. The GOS for excitations to $3s[3/2]_1+3s'[1/2]_1$. The inset graph shows the enlarged result near the minimum.

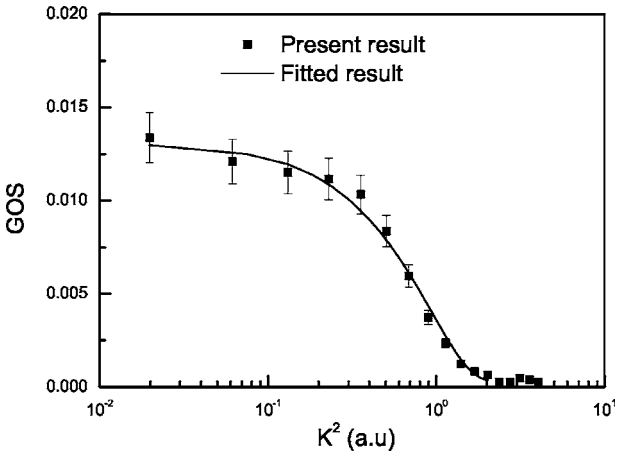

FIG. 5. The GOS for the electric dipole excitation to $4s[3/2]_1$.

of the impact energy, while for $3s[3/2]_1$, due to the low cross section, the maximum was not reported by Suzuki *et al.* [11]. This suggests that the first Born approximation is not reached in the large-K^2 region.

The sum of the GOS's for the excitations to $3s[3/2]_1$ and $3s[1/2]_1$ are shown in Fig. 4 and compared with the previous experimental and theoretical works [11,12,17]. The experimental result of Wong *et al.* was digitized from Ref. [12] and the theoretical one of Chen and Msezane was digitized from Ref. [17]. The relative GOS of Wong *et al.* was normalized to the present data at $K^2=1.132$ a.u. It can be seen that the result of Wong *et al.* measured at an incident electron energy of 25 keV has obvious differences with the present one in the large-K^2 region. This may be attributed to that the pressure effect was not corrected in their work [12]. In order to compare the present GOS profile with the previous theoretical calculation, the influence of the angular resolution must be considered, especially for the GOS's near the position of the extremum. Here the angular response function $A(u)$ is considered as a Gauss function, $A(u)=1/(\sqrt{2\pi}\alpha)\exp[-u^2/(2\alpha^2)]$, where $\alpha=\Delta\theta/\sqrt{8\ln 2}$ and $\Delta\theta$ is the present instrumental angular resolution 0.8° (FWHM). The theoretical result of Chen and Msezane [17] was convoluted with the present angular response function $A(u)$, and then the convoluted result was normalized to the present data at $K^2=2.357$ a.u., as shown in Fig. 4. It can be seen that the angular resolution has great influence on the GOS profile near the position of the minimum. The positions of the minimum and maximum of the GOS for excitations to $3s[3/2]_1+3s'[1/2]_1$ are listed in Table III. It can be seen that the position of the minimum for the convoluted result is in good agreement with the present one. However, we notice that the experimental and theoretical positions of the maximum [12,17,38] are all larger than the present results.

The GOS's for the excitations to $4s[3/2]_1$ and $4s'[1/2]_1$ are listed in Table II and shown in Figs. 5 and 6, respectively. The lines in Figs. 5 and 6 are the fitted results using Eq. (3). It can be seen that the profiles are typical ones for dipole-allowed transitions. The positions of the extrema for the two excitations are listed in Table IV.

The GOS's for the electric monopole transition to $3p'[1/2]_0$ are shown in Fig. 7 along with previous experimental results [11] and theoretical calculations [18]. In the region of $K^2<0.1$ a.u., the amplitude of the present GOS is lower than the experimental ones for low incident electron energies, while the theoretical result is higher than all the experimental ones. In the region of $K^2>0.1$ a.u., the amplitude and maximum position of the GOS increase with increasing of the incident electron energy and the theoretical position of the maximum is larger than all the experimental ones. This may indicate that the first Born approximation is not reached for the present result. It is interesting that the present GOS profile has only one maximum in the present K^2 region, which is different from experimental ones at low impact energies but in agreement with the theoretical calculation.

The GOS's for electric quadrupole excitations to $3p[5/2,3/2]_2+3p'[3/2]_2$ are shown in Fig. 8 along with the theoretical result (the dash-dotted line is the convoluted result) [18]. The amplitude and position of the first maximum

TABLE III. The positions of the minimum and maximum for GOS's of $2p^6\rightarrow 2p^5(3s+3s')$ transitions of Ne.

	Experimental		Theoretical		
K^2 (a.u.)	Present	Ref. [12]	Ref. [17]	Convoluted results [17]	Ref. [38]
Minimum	2.52±0.05	2.657	2.586	2.634	4.162
Maximum	3.47±0.1	7.398	6.554		11.492

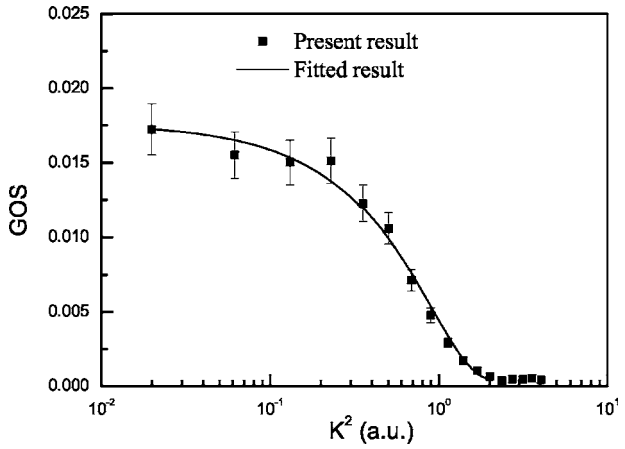

FIG. 6. The GOS for the electric dipole excitation to $4s'[1/2]_1$.

for the convoluted result are generally consistent with the present one except for the amplitude in the low-K^2 region. The positions of the maxima and the data of the GOS's for the electric monopole and electric quadrupole transitions are listed in Tables IV and II, respectively.

In addition, from our recent work [6] it is known that the GOS ratio can serve as a direct and rigorous test of the wave functions for excited states. Here the GOS ratios between the excitations to $4s[3/2]_1$ and $4s'[1/2]_1$ are shown in Fig. 9. It can be seen that the experimental GOS ratios are in agreement with the calculated composite coefficient square ratio (CCSR) of $E_1\alpha_1^2/E_2\alpha_2^2$ (E_1 and E_2 are the excitation energies, and α_1 and α_2 are the corresponding intermediate-coupling coefficients of the same singlet components, respectively) except for near the position of the GOS minimum. A detailed explanation can be found in our recent work [6]. Furthermore, using the mean value of the experimental GOS ratios ($0.782=E_1\alpha_1^2/E_2\alpha_2^2$) and the normalizing character for the intermediate-coupling coefficient ($\alpha_1^2+\alpha_2^2=1$) [6], the experimental intermediate-coupling coefficients for excitations to $4s[3/2]_1$ and $4s'[1/2]_1$ can be determined. The results are

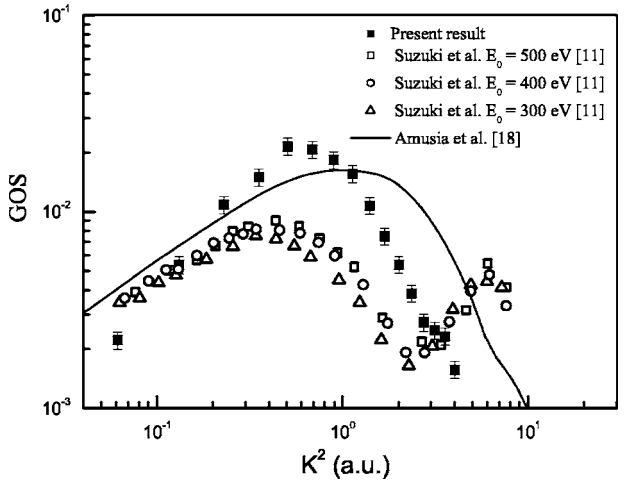

FIG. 7. The GOS for the electric monopole excitation to $3p'[1/2]_0$.

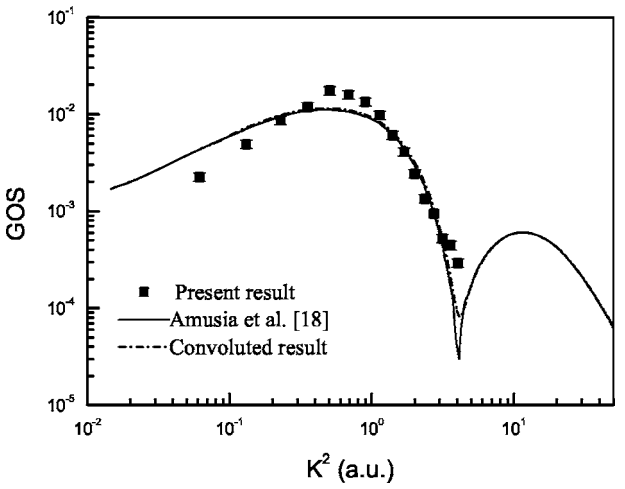

FIG. 8. The GOS for the electric quadrupole excitations to $3p[5/2,3/2]_2+3p'[3/2]_2$.

0.662 and 0.749, respectively, which are in good agreement with the calculated values of 0.675 and 0.737.

IV. SUMMARY AND CONCLUSION

The GOS's and positions of the extrema for excitations to $2p^53s$, $2p^53p$, and $2p^54s$ of Ne have been determined at the incident electron energy of 2500 eV using the method of a mixed gas of helium and neon. The excitations can be classified as electric monopole, electric dipole, and electric quadrupole transitions with the help of our calculated intermediate-coupling coefficients. In addition, the GOS ratios between excitations to $4s[3/2]_1$ and $4s'[1/2]_1$ and the experimental intermediate-coupling coefficients (the singlet component) for the two excitations were determined.

It is shown that the present minimum position for the GOS of the electric dipole excitations to $3s[3/2]_1+3s'[1/2]_1$ is in good agreement with the theoretical calculation by Chen and Msezane [17]. However, for the maximum there is an obvious difference between the present re-

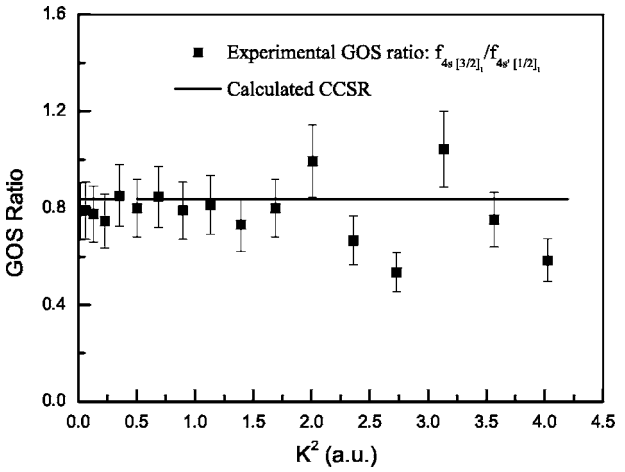

FIG. 9. The GOS ratios between excitations to $4s[3/2]_1$ and $4s'[1/2]_1$.

TABLE IV. The positions of the minimum and maximum for GOS's of $2p^6 \rightarrow 2p^5(4s,4s',3p)$ transitions of Ne.

			$3p'[1/2]_0$		$3p[5/2,3/2]_2+3p'[3/2]_2$	
K^2 (a.u.)	$4s[3/2]_1$	$4s'[1/2]_1$	Present	Theoretical [18]	Present	Theoretical [18]
Minimum	2.6±0.1	2.52±0.1				
Maximum	3.23±0.1	3.4±0.1	0.615±0.05	1.0	0.589±0.05	0.51

sult with other experimental and theoretical ones. Furthermore, the GOS profiles for the electric monopole excitation to $3p'[1/2]_0$ and electric quadrupole excitations to $3p[5/2,3/2]_2+3p'[3/2]_2$ are in general agreement with the theoretical calculations by Amusia *et al.* [18], while for the electric monopole excitation, the GOS measured by Suzuki *et al.* [11] has two maxima, which is different from the theoretical and present results. So further experimental and theoretical investigations of electric monopole, electric dipole, and electric quadrupole excitations are recommended.

ACKNOWLEDGMENTS

Support of this work by the National Nature Science Foundation of China (Grant Nos. 10474089 and 10134010) is gratefully acknowledged.

[1] D. L. Matthews, P. L. Hagelstein, M. D. Rosen, M. J. Eckart, N. M. Ceglio, A. U. Hazi, H. Medecki, B. J. MacGowan, J. E. Trebes, B. L. Whitten, E. M. Campbell, C. W. Hatcher, A. M. Hawryluk, R. L. Kauffman, L. D. Pleasance, G. Rambach, J. H. Scofield, G. Stone, and T. A. Weaver, Phys. Rev. Lett. **54**, 110 (1985).
[2] G. J. Tallents, J. Phys. D **36**, R259 (2003).
[3] C. C. Turci, J. T. Francis, T. Tyliszczak, G. G. de Souza, and A. P. Hitchcock, Phys. Rev. A **52**, 4678 (1995).
[4] X. J. Liu, L. F. Zhu, Z. S. Yuan, W. B. Li, H. D. Cheng, Y. P. Huang, Z. P. Zhong, K. Z. Xu, and J. M. Li, Phys. Rev. Lett. **91**, 193203 (2003).
[5] Y. K. Kim, M. Inokuti, G. E. Chamberlain, and S. R. Mielczarek, Phys. Rev. Lett. **21**, 1146 (1968).
[6] H. D. Cheng, L. F. Zhu, X. J. Liu, Z. S. Yuan, W. B. Li, and K. Z. Xu, Phys. Rev. A **71**, 032714 (2005).
[7] D. F. Register, S. Trajmar, G. Steffensen, and D. C. Cartwright, Phys. Rev. A **29**, 1793 (1984).
[8] M. A. Khakoo, T. Tran, D. Bordelon, and G. Csanak, Phys. Rev. A **45**, 219 (1992).
[9] M. A. Khakoo, C. E. Beckmann, S. Trajmar, and G. Csanak, J. Phys. B **27**, 3159 (1994).
[10] M. A. Khakoo, J. Wrkich, M. Larsen, G. Kleiban, I. Kanik, S. Trajmar, M. J. Brunger, P. J. O. Teubner, A. Crowe, C. J. Fontes, R. E. H. Clark, V. Zeman, K. Bartschat, D. H. Madison, R. Srivastava, and A. D. Stauffer, Phys. Rev. A **65**, 062711 (2002).
[11] T. Y. Suzuki, H. Suzuki, S. Ohtani, B. S. Min, T. Takayanagi, and K. Wakiya, Phys. Rev. A **49**, 4578 (1994).
[12] T. C. Wong, J. S. Lee, and R. A. Bonham, Phys. Rev. A **11**, 1963 (1975).
[13] P. S. Ganas and A. E. S. Green, Phys. Rev. A **4**, 182 (1971).
[14] T. Sawada, J. E. Purcell, and A. E. S. Green, Phys. Rev. A **4**, 193 (1971).
[15] L. E. Machado, E. P. Leal, and G. Csanak, Phys. Rev. A **29**, 1811 (1984).
[16] K. Bartschat and D. H. Madison, J. Phys. B **25**, 4619 (1992).
[17] Z. F. Chen and A. Z. Msezane, J. Phys. B **33**, 5397 (2000).
[18] M. Y. Amusia, L. V. Chernysheva, Z. Felfli, and A. Z. Msezane, Phys. Rev. A **67**, 022703 (2003).
[19] M. Inokuti, Rev. Mod. Phys. **43**, 297 (1971).
[20] H. Bethe, Ann. Phys. **5**, 325 (1930); Z. Phys. **76**, 293 (1930).
[21] B. G. Tian and J. M. Li, Acta Phys. Sin. **33**, 1401 (1984).
[22] J. J. Abdallah, R. E. H. Clark, and R. D. Cowan (unpublished).
[23] S. L. Wu, Z. P. Zhong, R. F. Feng, S. L. Xing, B. X. Yang, and K. Z. Xu, Phys. Rev. A **51**, 4494 (1995).
[24] K. Z. Xu, *et al.*, Phys. Rev. A **53**, 3081 (1996).
[25] X. J. Liu, L. F. Zhu, X. M. Jiang, Z. S. Yuan, B. Cai, X. J. Chen, and K. Z. Xu, Rev. Sci. Instrum. **72**, 3357 (2001).
[26] W. B. Li, L. F. Zhu, X. J. Liu, Z. S. Yuan, J. M. Sun, H. D. Cheng, Z. P. Zhong, and K. Z. Xu, Phys. Rev. A **67**, 062708 (2003).
[27] L. F. Zhu, X. J. Liu, W. B. Li, Z. S. Yuan, H. D. Cheng, Z. P. Zhong, and K. Z. Xu, Nucl. Phys. Rev. **19**, 150 (2002).
[28] L. F. Zhu, Z. P. Zhong, X. J. Liu, R. F. Feng, X. J. Zhang, and K. Z. Xu, J. Phys. B **32**, 4897 (1999).
[29] N. M. Cann and A. J. Thakkar, J. Electron Spectrosc. Relat. Phenom. **123**, 143 (2002).
[30] X. J. Liu, L. F. Zhu, Z. S. Yuan, W. B. Li, H. D. Cheng, J. M. Sun, and K. Z. Xu, J. Electron Spectrosc. Relat. Phenom. **135**, 15 (2004).
[31] E. N. Lassettre, J. Chem. Phys. **43**, 4479 (1965); K. N. Klump and E. N. Lassettre, *ibid.* **68**, 886 (1978).
[32] Z. P. Zhong, S. L. Wu, R. F. Feng, B. X. Yang, Q. Ji, K. Z. Xu, Y. Zou, and J. M. Li, Phys. Rev. A **55**, 3388 (1997).
[33] R. E. H. Clark, J. Abdallah, Jr., G. Csanak, and S. P. Kramer, Phys. Rev. A **40**, 2935 (1989).
[34] R. E. H. Clark, G. Csanak, and J. Abdallah, Jr., Phys. Rev. A **44**, 2874 (1991).
[35] C. E. Moore, *Atomic Energy Levels* (U.S. GPO, Washington, DC, 1971), Vol. 2.
[36] R. D. Cowan, *The Theory of Atomic Structure and Spectra* (University of California Press, Berkeley, CA, 1981).
[37] W. F. Chan, G. Cooper, X. Guo, and C. E. Brion, Phys. Rev. A **45**, 1420 (1992).
[38] K. J. Miller, J. Chem. Phys. **59**, 5639 (1973).